IEEE Photonics Journal
An IEEE Photonics Society Publication

Open Access

Dual-Polarization Dual-Parallel MZM and Optical Phase Shifter Based Microwave Photonic Phase Controller

Volume 8, Number 4, August 2016

T. Niu
X. Wang
E. H. W. Chan, Senior Member, IEEE
X. Feng
B. O. Guan

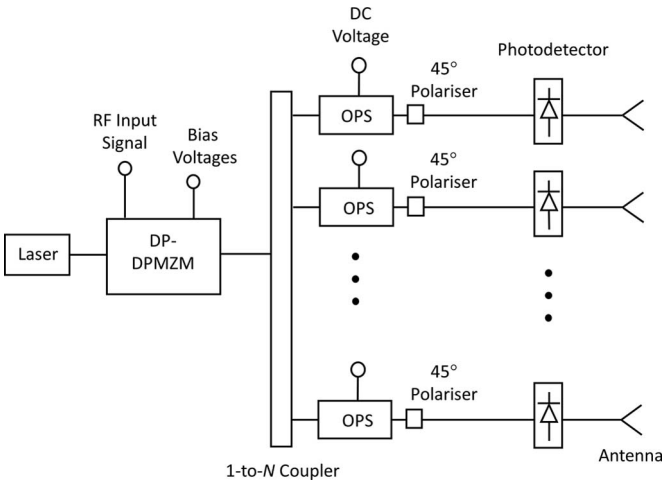

DOI: 10.1109/JPHOT.2016.2593584
1943-0655

IEEE photonics SOCIETY

IEEE

Dual-Polarization Dual-Parallel MZM and Optical Phase Shifter Based Microwave Photonic Phase Controller

T. Niu,[1] X. Wang,[1] E. H. W. Chan,[2] *Senior Member, IEEE*, X. Feng,[1] and B. O. Guan[1]

[1]Guangdong Provincial Key Laboratory of Optical Fiber Sensing and Communications, Institute of Photonics Technology, Jinan University, Guangzhou 510632, China
[2]School of Engineering and Information Technology, Charles Darwin University, Darwin, NT 0909, Australia

DOI: 10.1109/JPHOT.2016.2593584

Manuscript received June 21, 2016; revised July 14, 2016; accepted July 18, 2016. Date of publication July 20, 2016; date of current version August 1, 2016. This work was supported by the National Natural Science Foundation of China under Grant 61501205 and Grant 61475065; by the Fundamental Research Funds for the Central Universities under Grant 21615325; and by the Guangdong Natural Science Foundation under Grant 2015A030313322, Grant 2014A030310419, and Grant S2013030013302. Corresponding author: X. Wang (e-mail: txudong.wang@email.jnu.edu.cn).

Abstract: A new microwave photonic phase controlling structure that can realize a continuously tunable 0° to 360° phase shift using only one DC voltage control is presented. Unlike other phase controlling structures, the radio-frequency (RF) signal phase shift produced by the new phase controller has a predefined linear relationship with the control voltage. This enables users to easily determine the control voltage needed to realize the desired RF signal phase shift. The microwave photonic phase controller is based on an integrated dual-polarization dual-parallel Mach–Zehnder modulator (DPMZM) and a polarization-dependent optical phase shifter. It is suitable for realizing multiple RF signal phase shifts, which are required in beamforming applications. Experimental results are presented which demonstrate the realization of a continuously tunable −180° to 180° phase shift with little phase and amplitude variations over a wide frequency range, as well as a linear RF signal phase shift to control voltage relationship.

Index Terms: Microwave phase controller, microwave photonics, wideband phase controllers, phased-array antennas.

1. Introduction

Beamforming is a spatial filtering technique for transmitting or receiving signals illuminating an array of sensors from some specific directions while attenuating signals from other directions [1]. A common example is a phased-array antenna system, which consists of a group of multiple active antennas coupled to a common source or load to produce a directive radiation pattern, and has the benefits of fast scanning, the elimination of mechanical complexity and reliability issues, and the ability to host multiple beams on the same array. The direction of the radiation pattern generated by a phased-array antenna can be controlled using phase controllers. Typical phased-array antenna systems used in radar defense applications require a large number of phase controllers. Each phase controller needs to provide a tunable 0° to 360° phase shift with constant output radio-frequency (RF) signal amplitude over the system bandwidth. Currently, microwave

phase controllers are implemented using ferrite materials, p-i-n diodes, or field effect transistor (FET) switches [2]. Microwave phase controlling techniques such as those based on monolithic microwave integrated circuits (MMICs) [3], microelectromechanical systems (MEMS) [2], active vector modulator [4], and variable resonant circuits [5] have been reported. However, they have limited tuning resolution, have a limited phase shift range, require multiple controls, or require high DC power. Furthermore, all of them have limited bandwidth. Recently, an active phase controller based on 0.18 μm SiGe BiCMOS technology have been demonstrated to achieve 0° to 360° phase shift in 6 GHz to 18 GHz frequency range, but its resolution is limited to 5 bits and has around 4 dB changes in the output RF signal amplitude during the phase shifting operation [6].

Photonics provides a promising solution to overcome the limitations in conventional microwave phase controllers. Processing microwave signals in the photonic domain also has the benefits of excellent isolation, electromagnetic interference immunity and remote antenna feeding [7]. Various microwave photonic phase controllers have been reported [8]–[22]. Some require multiple controls to realize full 0° to 360° RF signal phase shift without large changes in the output RF signal amplitude, e.g., controlling two bias voltages into a dual-parallel Mach–Zehnder modulator (DPMZM) [8], adjusting the wavelengths of two RF phase modulated optical signals into a nonlinear phase response optical filter [9], controlling the probe and pump laser power into a highly nonlinear fiber [10], and controlling two optical switches and optical attenuators at the dual-output Mach–Zehnder modulator outputs [11]. A single-control RF phase controller is of interest since it reduces the phase shifting operation complexity. The reported microwave photonic phase controllers that require only a single control to shift the RF signal phase either have a limited bandwidth [12]; have a complex structure requiring a long length of fiber, which increases the system size and weight [13], [14]; cannot achieve full 0° to 360° phase shift [15]; require a programmable photonic processor comprising a 2-D array of liquid crystal on silicon pixels [16], [17], which is expensive and has a slow response time; rely on using a polarization controller to adjust the light polarization state [18], which does not have a simple predefined relationship between the RF signal phase shift and the polarization controller adjustment; perform the phase shifting operation and the RF signal modulation on the same device, e.g., a DPMZM [19], which is not practical for beamforming applications as multiple phase shifts require multiple broadband DPMZMs.

In this paper, we present a new microwave photonic phase controller that only needs one control voltage to achieve full 0° to 360° RF phase shift in a wide range of frequency. The concept is based on employing a commercially available integrated dual-polarization dual-parallel Mach–Zehnder modulator (DP-DPMZM) to realize a single sideband (SSB) RF modulated optical signal in which the optical carrier and the sideband are in an orthogonal polarization state, together with a polarization dependent optical phase shifter (OPS) to control the optical phase difference between the sideband and the carrier. It has a simple structure, a high phase shift resolution and a fast tuning time. The phase controller can also be controlled in a remote location. Experimental results are presented demonstrating the RF phase tuning capabilities for beamforming applications and the phase controller has a linear control voltage to RF signal phase shift relationship.

2. Phase Controller Principle of Operation

The operation of the new microwave photonic phase controller structure is based on introducing an optical phase difference between a single RF modulation sideband and an optical carrier and converting this optical phase difference into an RF signal phase shift when the sideband and carrier beat at the photodetector. Most of the reported microwave photonic phase controllers operate on this principle. However, they have a complex structure and/or other limitations such as slow tuning time, high cost and difficult to control, which make them not suitable for use in phased-array antenna systems that have a large number of phase controllers. The new microwave photonic phase controller structure shown in Fig. 1 provides a solution to these problems. It consists of an integrated DP-DPMZM for RF signal modulation

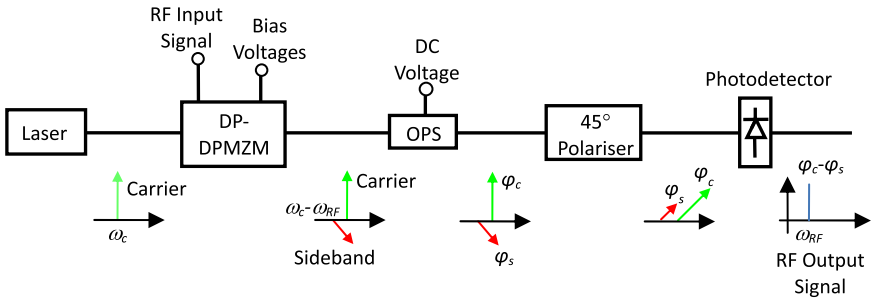

Fig. 1. New microwave photonic phase controller.

and a polarization dependent OPS with a 45° polarizer. The light from the optical source is modulated by an integrated DP-DPMZM driven by an input RF signal. By designing the modulator bias voltages, a SSB RF modulated optical signal where the RF modulation sideband and optical carrier are in an orthogonal polarization state, can be obtained at the modulator output. The spectrum of the SSB RF modulated optical signal is also shown in Fig. 1. The two orthogonal polarization components pass through a polarization dependent OPS, which introduces different optical phases to the sideband and carrier by changing the DC voltage into the OPS. A 45° angle linear polarizer connected after the OPS converts the polarization state of the RF modulation sideband and the optical carrier to have the same polarization state with a 45° angle to the slow axis. The sideband and carrier having the same polarization state beat at the photodiode to generate an RF signal with the phase the same as the sideband and carrier optical phase difference. Note that the DP-DPMZM is an electro-optic device like a normal MZM used for RF signal modulation therefore it is polarization sensitive and hence a polarization maintaining fibre is needed between the laser source and the DP-DPMZM. Like many microwave photonic phase controllers [10]–[15], [18], polarization maintaining components are required to implement the DP-DPMZM and OPS based microwave photonic phase controller in order to obtain a stable output that is insensitive to changes in light polarization state. In the case where the phase control function is performed at the transmitter, the DP-DPMZM, the OPS and the 45° polarizer can be integrated together to avoid light polarization state changes between these components. In the case where the phase control function is performed in a remote location, a polarization maintaining fibre is needed to connect between the DP-DPMZM and the OPS. Alternatively a normal single mode fibre can be used with a polarization stabilizer [24] at the OPS input to fixed and align the carrier and sideband polarization state to the slow and fast axis respectively.

The DP-DPMZM is formed by two DPMZMs, a 90° polarization rotator followed by a polarization beam combiner (PBC), as shown in Fig. 2(a). Each DPMZM contains two MZMs. It has two RF input ports and three bias ports. A single sideband suppressed carrier (SSB-SC) RF modulated optical signal can be generated by designing the modulator bias voltages. Detailed discussion on the structure and the operation principle of a DPMZM for SSB-SC modulation can be found in [23]. A pair of RF signals with 90° phase difference is fed into the RF input ports of the lower DPMZM in the DP-DPMZM. The modulator bias voltages (V_{b1}, V_{b2} and V_{b3}) are designed to suppress both the right sideband and the optical carrier leaving only the left sideband at the lower DPMZM output. No RF signal is applied to the upper DPMZM. The bias voltages (V_{b4}, V_{b5} and V_{b6}) of this DPMZM are designed to minimize the loss of the light passing through this modulator. The bias voltages of the two DPMZMs required to obtain the above operation condition are given in the next section. The polarization state of the light at the lower DPMZM output is rotated by 90° via a 90° polarization rotator. The output of the DPMZM in the upper arm and the output of the 90° polarization rotator in the lower arm are combined via a PBC generating an orthogonally polarized sideband and carrier at the output of the DP-DPMZM. The polarization state of the sideband and carrier at the DP-DPMZM output are aligned to the fast and slow axis, respectively, as shown in Fig. 2(c). It should be

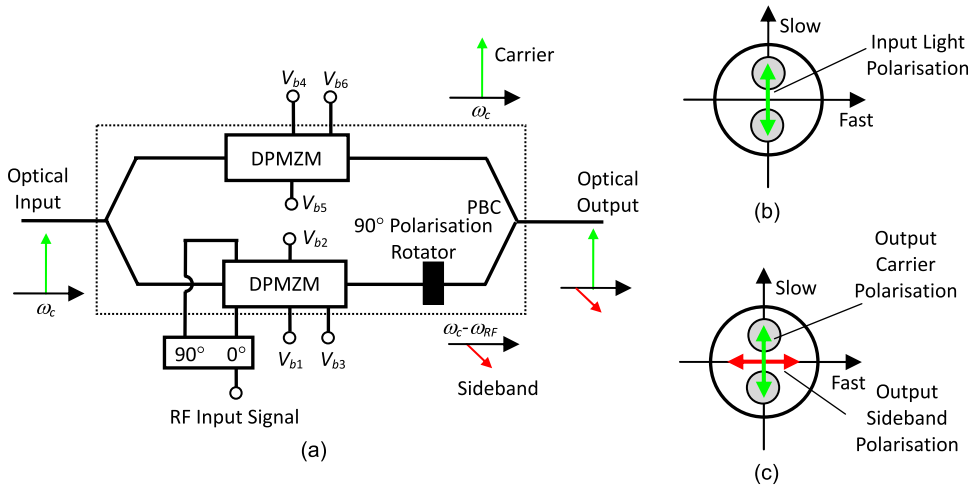

Fig. 2. (a) Structure of the integrated DP-DPMZM where the lower DPMZM is driven by a pair of 90° phase difference RF signals. Polarization direction of the light at the (b) input and (c) output of the DP-DPMZM.

pointed out that the DPMZM in the upper arm of the DP-DPMZM can be eliminated as it simply allows the light from the modulator input to be passed to the modulator output. However, an optical modulator formed by an upper direct path and a lower path consists of a DPMZM needs to be custom made. On the other hand, a DP-DPMZM is commercially available from manufacturers such as Fujitsu, which is used for dual-polarization quadrature phase shift keying (DP-QPSK) transmission.

Note that a single modulator bias controller instead of multiple DC power supplies can be used to provide six bias voltages for the DP-DPMZM. The bias controller from PlugTech [25] is very compact and low cost. It allows the modulators inside the DP-DPMZM to be biased at any transmission point defined by the user. The modulator operating points are fixed by the bias controller, which has a fast response time to ensure the system has a stable performance. The OPS formed by a Z-cut Lithium Niobate crystal ($LiNbO_3$) is a polarization dependent device. It is capable of supporting light travels in both the transverse magnetic (TM) mode and the transverse electric (TE) mode. The optical phase shift efficiencies for the two modes are different. When the polarization states of the sideband and carrier in the fast and slow axis are aligned with the TE and TM modes, different optical phases of φ_s and φ_c are introduced to the sideband and carrier respectively, and the optical phase difference between the sideband and carrier $\varphi_c - \varphi_s$ can be tuned by changing the DC voltage into the polarization dependent OPS. Note that the optical phase change in $LiNbO_3$ is due to the Pockels effect, which is a change in the refractive index or birefringence that depends linearly on the electric field applied to the modulator [26]. Thus the phase controller output RF signal phase, which is equal to the optical phase difference $\varphi_c - \varphi_s$, has a linear relationship with the DC voltage into the polarization dependent OPS.

3. Analysis

When a DPMZM is driven by a pair of 90° phase difference RF signals, the DPMZM output electric field can be written as

$$E_{\text{out,DPMZM}} = \frac{E_{\text{in,DPMZM}}}{2}\sqrt{L_{\text{DPMZM}}}\left(Ae^{j(\omega_c t+\alpha)} + Be^{j((\omega_c+\omega_{RF})t+\beta)} + Ce^{j((\omega_c-\omega_{RF})t+\gamma)}\right) \quad (1)$$

where $E_{\text{in,DPMZM}}$ and ω_c are the electric field amplitude and angular frequency of the light at the DPMZM input, respectively; ω_{RF} is the angular frequency of the input RF signal; L_{DPMZM} is the

DPMZM insertion loss; A, B, C, α, β, and γ are the amplitudes and phases of the carrier, right sideband, and left sideband, respectively, and are given by

$$A = \sqrt{(\cos\varphi_1 + \cos\varphi_2 \cos\varphi_3)^2 + (\cos\varphi_2 \sin\varphi_3)^2} \tag{2}$$

$$B = J_1(\beta_{RF})\sqrt{(-\sin\varphi_2 \cos\varphi_3)^2 + (\sin\varphi_1 - \sin\varphi_2 \sin\varphi_3)^2} \tag{3}$$

$$C = J_1(\beta_{RF})\sqrt{(-\sin\varphi_2 \cos\varphi_3)^2 + (-\sin\varphi_1 - \sin\varphi_2 \sin\varphi_3)^2} \tag{4}$$

$$\alpha = tan^{-1}\left(\frac{\cos\varphi_2 \sin\varphi_3}{\cos\varphi_1 + \cos\varphi_2 \cos\varphi_3}\right) \tag{5}$$

$$\beta = tan^{-1}\left(\frac{\sin\varphi_1 - \sin\varphi_2 \sin\varphi_3}{-\sin\varphi_2 \cos\varphi_3}\right) \tag{6}$$

$$\gamma = tan^{-1}\left(\frac{-\sin\varphi_1 - \sin\varphi_2 \sin\varphi_3}{-\sin\varphi_2 \cos\varphi_3}\right) \tag{7}$$

where $J_m(x)$ is the Bessel function of mth order of first kind, $\beta_{\mathrm{RF}} = \pi V_{\mathrm{RF}}/V_\pi$ is the modulation index, V_{RF} is the input RF signal amplitude, V_π is the modulator half wave voltage, and $\varphi_n = \pi V_{bn}/V_\pi$ is the optical phase change introduced by the bias voltage V_{bn} into the DPMZM. In order to suppress the right sideband and the carrier so that only the left sideband appears at the modulator output, the conditions where $A = B = 0$ and $C \neq 0$ need to be satisfied. This requires $\varphi_1 = \varphi_2 = \varphi_3 = \pi/2$ as can be seen from (2)–(4), which can be obtained by setting the modulator bias voltages $V_{b1} = V_{b2} = V_{b3} = V_\pi/2$. Under this condition, (1) can be rewritten as

$$E_{\mathrm{out,DPMZM}} = E_{\mathrm{in,DPMZM}}\sqrt{L_{\mathrm{DPMZM}}} \cdot J_1(\beta_{\mathrm{RF}})e^{j((\omega_c - \omega_{\mathrm{RF}})t - \pi/2)}. \tag{8}$$

When there is no RF signal at the DPMZM input, the DPMZM output electric field can be written as

$$E_{\mathrm{out,DPMZM}} = \frac{E_{\mathrm{in,DPMZM}}}{2}\sqrt{L_{\mathrm{DPMZM}}}Ae^{j(\omega_c t + \alpha)}. \tag{9}$$

In order to maximize the amplitude of the optical carrier at the modulator output, V_{b1}, V_{b2} and V_{b3} are set to 0 so that $\varphi_1 = \varphi_2 = \varphi_3 = 0$. Therefore, (9) can be rewritten as

$$E_{\mathrm{out,DPMZM}} = E_{\mathrm{in,DPMZM}}\sqrt{L_{\mathrm{DPMZM}}}e^{j\omega_c t}. \tag{10}$$

With reference to the DP-DPMZM configuration shown in Fig. 2(a), when the light at the DP-DPMZM input is aligned to the slow axis and the modulator bias voltages $V_{b1} = V_{b2} = V_{b3} = V_\pi/2$ and $V_{b4} = V_{b5} = V_{b6} = 0$, the DP-DPMZM output electric field becomes

$$E_{\mathrm{out,DP-DPMZM}} = \frac{\sqrt{2}E_{in}}{2}\sqrt{L}\left(\hat{y}e^{j\omega_c t} + \hat{x}J_1(\beta_{\mathrm{RF}})e^{j((\omega_c - \omega_{\mathrm{RF}})t - \pi/2)}\right) \tag{11}$$

where E_{in} is the DP-DPMZM input electric field amplitude, L is the DP-DPMZM insertion loss, and $\hat{x}$ and $\hat{y}$ are the polarization states representing light travelling in the fast axis and slow axis respectively. Equation (11) shows the output of the DP-DPMZM contains a pair of orthogonally polarized left sideband and optical carrier. When the slow and fast axis at the output of the DP-DPMZM are aligned with the TM and TE modes of the $LiNbO_3$

crystal in the OPS, changing the DC voltage into the OPS introduces different optical phases to the left sideband and carrier. The OPS output electric field can be written as

$$E_{\text{out,OPS}} = \frac{\sqrt{2}E_{\text{in}}}{2}\sqrt{L'}\left(\hat{y}e^{j(\omega_c t+\varphi_c)} + \hat{x}J_1(\beta_{\text{RF}})e^{j((\omega_c-\omega_{\text{RF}})t-\pi/2+\varphi_s)}\right) \tag{12}$$

where L' is the total insertion loss of the DP-DPMZM and OPS, and φ_s and φ_c are the optical phase introduced by the polarization dependent OPS to the left sideband and optical carrier respectively. The electric field after a linear polarizer with a transmission axis at a 45° angle between the fast and slow axis, is given by

$$E_{\text{out,Pol}} = \frac{E_{\text{in}}\sqrt{L_{\text{total}}}}{2}\left(e^{j(\omega_c t+\varphi_c)} + J_1(\beta_{\text{RF}})e^{j((\omega_c-\omega_{\text{RF}})t-\pi/2+\varphi_s)}\right) \tag{13}$$

where L_{total} is the total insertion loss of the DP-DPMZM, OPS and polarizer. The microwave photonic phase controller output photocurrent at the RF signal frequency can be obtained from (13) and is written as

$$I_{\text{RF}} = \frac{1}{2}\Re L_{\text{total}}P_{\text{in}}J_1(\beta_{\text{RF}})\sin[\omega_{RF}t + (\varphi_c - \varphi_s)] \tag{14}$$

where $\Re$ is the photodiode responsivity, and P_{in} is the optical power into the DP-DPMZM.

Equation (14) shows the output RF signal phase can be controlled by varying the RF modulation sideband and the optical carrier phase difference. This can be obtained by changing the DC voltage into the polarization dependent OPS. A $LiNbO_3$ electro-optic phase modulator supporting light travelling in both TM and TE polarization states with different modulation efficiencies can be used to produce a polarization dependent optical phase shift. The relationship between the sideband and carrier optical phase difference, i.e. the RF signal phase shift produced by the microwave photonic phase controller, and the phase modulator input DC voltage V_{DC} can be written as

$$\varphi_c - \varphi_s = \frac{\pi V_{\text{DC}}}{V_{\pi,\text{PM}}}(1-\alpha) \tag{15}$$

where $V_{\pi,\text{PM}}$ is the phase modulator half wave voltage for light travelling in the TM polarization state, and α is the ratio of the TE to TM polarized light phase modulation efficiency. The value of α is mainly dependent on the $LiNbO_3$ electro-optic coefficient along the TE and TM axis, and can be varied in the range of 0.22 to 0.33 dependent on the sample of $LiNbO_3$ crystal that is used to implement the phase modulator [27], [28]. Equations (14) and (15) show the microwave photonic phase controller RF signal phase shift and the control voltage have a linear relationship. This is important as it allows users to design the required DC voltage to obtain an RF signal phase shift whereas similar relationship is not defined in conventional phase controlling structures, e.g., [18], which relies on a polarization controller adjustment to shift an RF signal phase. Note that altering the DC voltage into an electro-optic phase modulator only changes the sideband and carrier optical phase difference without affecting their amplitudes. Hence the DP-DPMZM and OPS based microwave photonic phase controller output RF signal amplitude remains constant while shifting the RF signal phase.

4. Simulation Results and Discussion

The phase controller structure was simulated using VPItransmissionMaker photonic simulation software [29]. The DP-DPMZM was set up using two DPMZMs having the same structure as shown in [23]. The outputs of the upper DPMZM and the lower DPMZM followed by a 90° polarization rotator were combined in a PBC. The lower DPMZM was driven by a pair of 90° phase difference RF signals whose frequency was swept from 0 to 40 GHz. The bias voltages of the two DPMZMs were set to obtain an orthogonally polarized single RF modulation sideband and

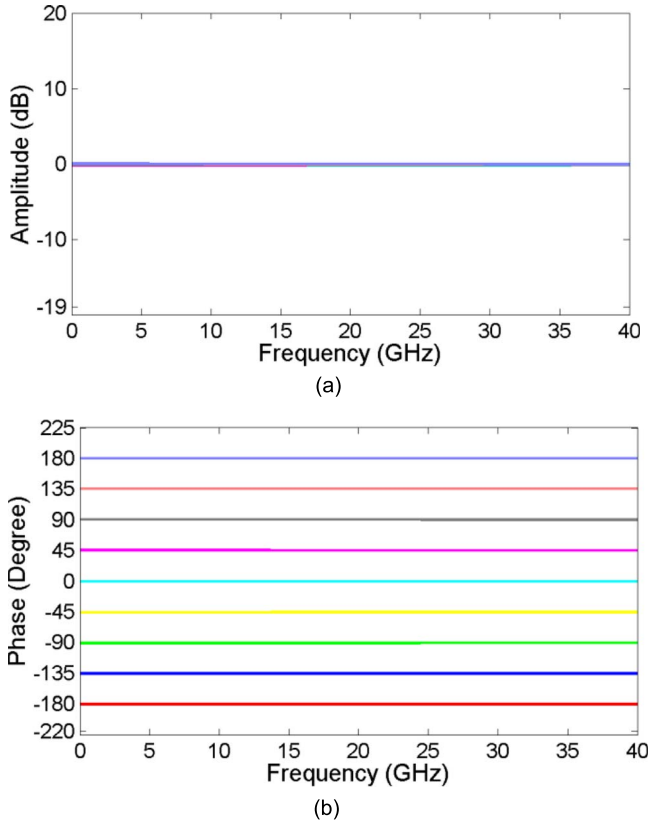

Fig. 3. VPI simulated (a) amplitude and (b) phase response of the microwave photonic phase controller for different DC voltages into a polarization-dependent OPS with a TE to TM polarized light phase modulation efficiency ratio α of 0.22.

optical carrier. A polarization dependent OPS was implemented by using a polarization beam splitter (PBS) to split the orthogonally polarized sideband and carrier, connecting the PBS outputs to two phase modulators with different modulation efficiencies, and using a PBC to combine the two phase modulator outputs. A linear polarizer with a 45° angle was connected after the polarization dependent OPS. The output RF signal was monitored on an RF spectrum analyzer connected to the photodetector output. Fig. 3 shows the amplitude and phase response of the microwave photonic phase controller for different DC voltages into the polarization dependent OPS. Fig. 3 shows that the phase of the output RF signal can be shifted over the full range from $-180°$ to 180° with no change in the output RF signal amplitude. The output RF signal phase shift versus the DC voltage into the polarization dependent OPS for different α values is shown in Fig. 4. A linear relationship can be seen. Note that a polarization dependent OPS with a different α value requires a slightly different DC voltage range to shift the output RF signal phase from $-180°$ to 180°. The RF signal modulation efficiency and the nonlinearity of the DP-DPMZM operated under the bias condition of the phase controller described in Section 2 were also investigated. VPItransmissionMaker simulation results show for the same input RF signal power and the same laser power into the modulators, the DP-DPMZM output RF signal power is smaller than that of the quadrature-biased MZM. One can increase the DP-DPMZM output RF signal power by increasing the modulation index, but this also increases the output third order harmonic component. However, simulation results show the ratio of the RF signal power to the third order harmonic component power at the DP-DPMZM output is similar to that of the quadrature-biased MZM when using a high modulation index.

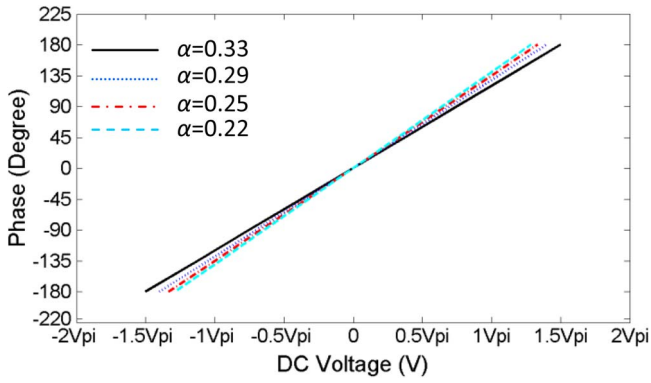

Fig. 4. VPI simulated RF phase shift versus DC voltage into the polarization-dependent OPS for different values of α.

In practice, a pair of 90° phase difference RF signals can be generated by employing a 90° hybrid coupler to split an RF signal into two with a 90° phase difference. Broadband 90° hybrid couplers are commercially available, e.g., a 3 dB 90° hybrid coupler from Marki Microwave has a bandwidth of 8 to 67 GHz [30], but have phase and amplitude imbalance in the two coupler outputs. The effect of the microwave photonic phase controller performance due to the coupler phase and amplitude imbalance was analyzed. Equations (16) and (17), shown below, show the phase controller output RF signal phase shift $\phi(\omega_{RF})$ and amplitude variation $K(\omega_{RF})$ with the inclusion of the 90° hybrid coupler phase and amplitude imbalance

$$\phi(\omega_{\mathrm{RF}}) = \tan^{-1}\left(\frac{Y(\omega_{\mathrm{RF}})}{X(\omega_{\mathrm{RF}})}\right) \tag{16}$$

$$K(\omega_{\mathrm{RF}}) = \sqrt{X(\omega_{\mathrm{RF}})^2 + Y(\omega_{\mathrm{RF}})^2} \tag{17}$$

where

$$\begin{aligned} X(\omega_{\mathrm{RF}}) = & -\sqrt{[-A(\omega_{\mathrm{RF}})\cos\theta(\omega_{\mathrm{RF}})]^2+[1-A(\omega_{\mathrm{RF}})\sin\theta(\omega_{\mathrm{RF}})]^2} \\ & \cdot \sin\left[\tan^{-1}\left(\frac{1-A(\omega_{\mathrm{RF}})\sin\theta(\omega_{\mathrm{RF}})}{-A(\omega_{\mathrm{RF}})\cos\theta(\omega_{\mathrm{RF}})}\right) - \varphi_c + \varphi_s\right] \\ & - \sqrt{[A(\omega_{\mathrm{RF}})\cos\theta(\omega_{\mathrm{RF}})]^2+[-1-A(\omega_{\mathrm{RF}})\sin\theta(\omega_{\mathrm{RF}})]^2} \\ & \cdot \sin\left[-tan^{-1}\left(\frac{-1-A(\omega_{\mathrm{RF}})\sin\theta(\omega_{\mathrm{RF}})}{A(\omega_{\mathrm{RF}})\cos\theta(\omega_{\mathrm{RF}})}\right) + \varphi_c - \varphi_s\right] \end{aligned} \tag{18}$$

$$\begin{aligned} Y(\omega_{\mathrm{RF}}) = & \sqrt{[-A(\omega_{\mathrm{RF}})\cos\theta(\omega_{\mathrm{RF}})]^2+[1-A(\omega_{\mathrm{RF}})\sin\theta(\omega_{\mathrm{RF}})]^2} \\ & \cdot \cos\left[\tan^{-1}\left(\frac{1-A(\omega_{\mathrm{RF}})\sin\theta(\omega_{\mathrm{RF}})}{-A(\omega_{\mathrm{RF}})\cos\theta(\omega_{\mathrm{RF}})}\right) - \varphi_c + \varphi_s\right] \\ & + \sqrt{[A(\omega_{\mathrm{RF}})\cos\theta(\omega_{\mathrm{RF}})]^2+[-1-A(\omega_{RF})\sin\theta(\omega_{\mathrm{RF}})]^2} \\ & \cdot \cos\left[-\tan^{-1}\left(\frac{-1-A(\omega_{\mathrm{RF}})\sin\theta(\omega_{\mathrm{RF}})}{A(\omega_{\mathrm{RF}})\cos\theta(\omega_{\mathrm{RF}})}\right) + \varphi_c - \varphi_s\right] \end{aligned} \tag{19}$$

where $\theta(\omega_{\mathrm{RF}})$ and $A(\omega_{\mathrm{RF}})$ are the 90° hybrid coupler phase and amplitude imbalance, respectively. Note that in the ideal case where the coupler has no phase imbalance and no amplitude imbalance, i.e. $\theta(\omega_{\mathrm{RF}}) = 90°$ and $A(\omega_{\mathrm{RF}}) = 1$, the microwave photonic phase controller RF signal phase shift and amplitude variation become $\phi(\omega_{RF}) = \phi_c - \phi_s$ and $K(\omega_{RF}) = 2$, indicating the phase controller has a constant amplitude. Equations (16)–(19) show, in practice, that the microwave photonic phase controller implemented using a 90° hybrid coupler has a frequency

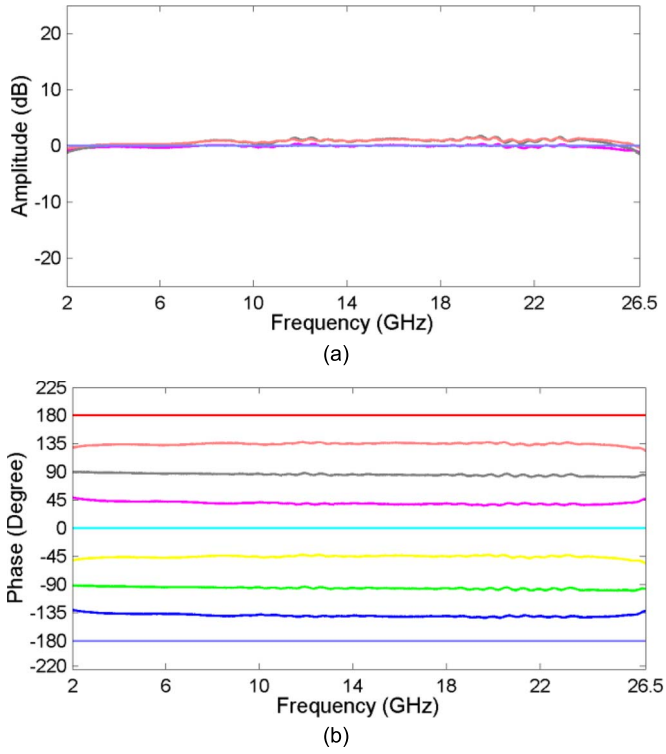

Fig. 5. Simulated microwave photonic phase controller (a) amplitude and (b) phase response with the inclusion of the amplitude and phase imbalance in a pair of 90° phase difference RF signals into the DP-DPMZM.

dependent amplitude and phase response performance. The phase and amplitude imbalance of a commercial 2–26.5 GHz bandwidth 90° hybrid coupler were measured to be ±4.3° and ±1.9 dB respectively. They were used together with (16)–(19) to simulate the performance of the DP-DPMZM and OPS based microwave photonic phase controller. The simulated phase controller amplitude and phase response shown in Fig. 5 reveal that there exist 7.2° and 3.3 dB phase and amplitude variation. This shows a 90° hybrid coupler with low phase and amplitude imbalance is needed for the phase controller to obtain a flat phase and amplitude response performance.

In addition to having a very easy control phase controlling operation, the phase controller shown in Fig. 1 has a simple structure and can be built using off-the-shelf components. Both the resolution and the response time of the phase controller are determined by the DC power supply that provides a control voltage into the polarization dependent OPS. Normal commercial DC power supplies have high < 10 mV voltage resolution and a fast < 50 μs response time. Therefore the DP-DPMZM and OPS based microwave photonic phase controller is able to obtain an RF signal phase shift with a 1° phase shift resolution and a tuning speed similar to that of the phase controllers which are based on controlling one or more DC voltages into an optical modulator to realize an RF signal phase shift [8], [19]. The phase modulator, which is used as a polarization dependent OPS, does not need to have a wide bandwidth. A polarizer can be integrated to the output port of the phase modulator to form a compact and low-cost device for RF phase controlling operation.

Note that the new microwave photonic phase controller can be extended to realize multiple RF signal phase shifts for use in phased array antennas as shown in Fig. 6. The 1-to-*N* coupler splits the orthogonally polarized single RF modulation sideband and optical carrier after the DP-DPMZM into *N* outputs. Each output is connected to a polarization dependent OPS followed by a 45° angle linear polarizer to shift an RF signal phase. Therefore *N* RF signal phase shifts only require *N* pairs of an OPS and a polarizer. This shows the realization of multiple RF signal

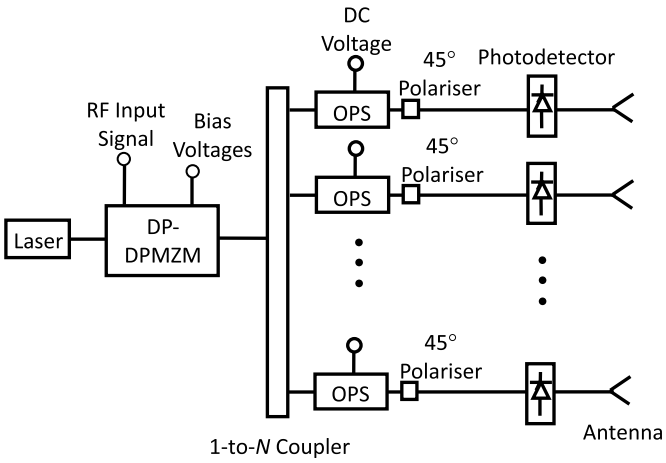

Fig. 6. Topology of the DP-DPMZM and OPS based microwave photonic phase controllers for realizing multiple RF phase controlling operation.

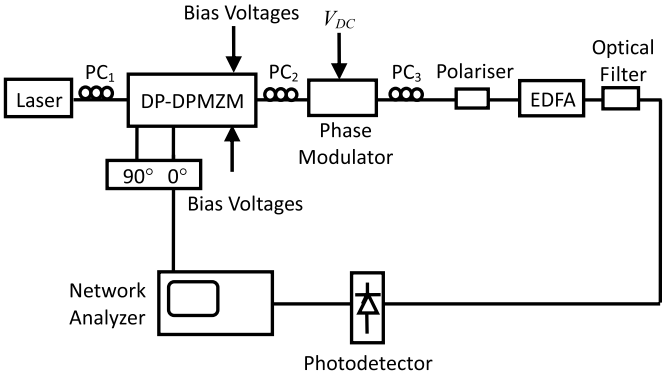

Fig. 7. DP-DPMZM and OPS based microwave photonic phase controller experimental setup.

phase shifts using the new phase controller structure is much simpler than other microwave photonic phase controllers such as those based on stimulated Brillouin scattering [13], [14] or those where the RF phase controlling operation and the RF signal modulation are performed on the same device [8], [19]. Note that microwave photonic phase controller structures for realizing multiple RF signal phase shifts have been reported [20]–[22]. However, they either require a wavelength tunable laser source or an electrical controlled polarization controller for each RF phase shift, which are expensive, and do not have a simple linear RF phase shift to control voltage relationship.

5. Experimental Results

Experiments were set up as shown in Fig. 7 to demonstrate the new microwave photonic phase controller. The optical source used in the experiment had a 1550 nm wavelength and 100 kHz linewidth. The DP-DPMZM was a commercial device from Fujitsu (FTM7977HQA). An optical phase modulator from Covega (Mach-10 053-10-S-A-A) was used as a polarization dependent OPS. It had a half wave voltage of 3.5 V. An erbium-doped fiber amplifier (EDFA) was connected to the polarizer output to compensate for the system loss. A 1 nm bandwidth optical filter after the EDFA was used to suppress the amplified spontaneous emission noise. The output optical signal was detected by a photodiode having a 50 GHz bandwidth.

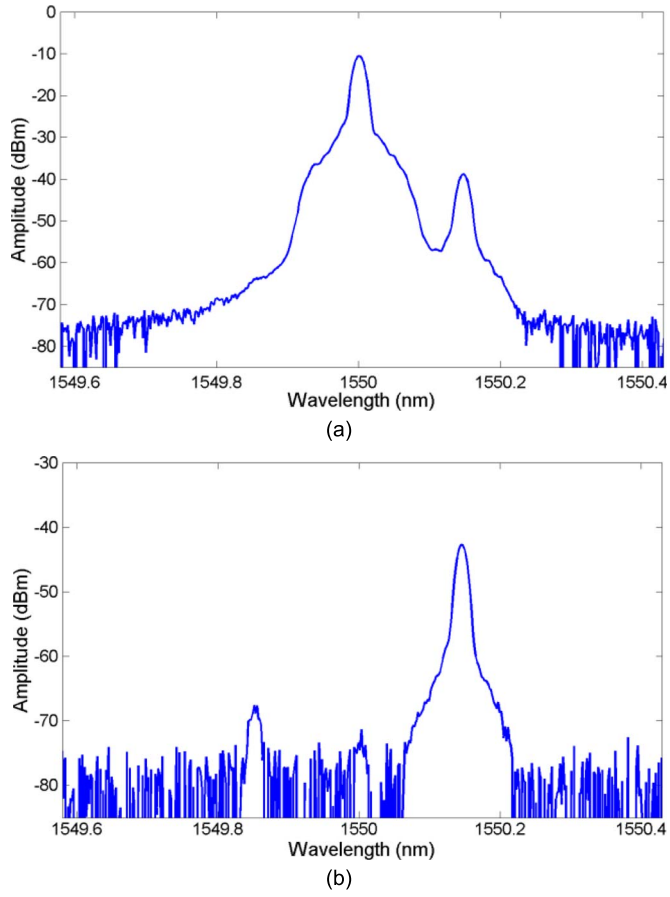

Fig. 8. (a) Optical spectrum at the output of the DP-DPMZM and (b) the optical spectrum at the output of the DP-DPMZM followed by a polarizer.

A 2–26.5 GHz bandwidth 90° hybrid coupler was used in the setup to demonstrate the RF phase controlling operation. The DP-DPMZM output optical spectrum, when the lower DPMZM inside the DP-DPMZM was driven by an 18 GHz RF signal, was measured on an optical spectrum analyzer (OSA), as shown in Fig. 8(a), in which the left sideband has been suppressed leaving only the right sideband and the carrier. Note that the horizontal axis on the OSA display is in wavelength. Therefore a right sideband in wavelength corresponds to a left sideband in frequency. In order to verify the right sideband and the carrier in Fig. 8(a) have an orthogonal polarization state, a polarizer was connected at the DP-DPMZM output after PC_2. The polarization state of the right sideband was adjusted via PC_2 to align with the polarizer transmission axis, and the polarizer output optical spectrum is shown in Fig. 8(b). The figure reveals the optical carrier is largely suppressed while the right sideband is reduced by only around 3 dB, which is caused by the insertion loss of PC_2 and the polarizer. This shows the carrier from the upper DPMZM of the DP-DPMZM and the right sideband from the lower DPMZM have an orthogonal polarization state. Note that the undesired component at 1549.85 nm wavelength is the left sideband, which has the same polarization state as the right sideband and cannot be fully suppressed due to the non-ideal characteristic of the DPMZM and the 90° hybrid coupler. However, this undesired component is more than 25 dB and 50 dB below the sideband and carrier at the DP-DPMZM output respectively, which has a negligible effect to the phase controller.

The amplitude and phase response of the microwave photonic phase controller were measured from 2 GHz to 26.5 GHz for different DC voltages V_{DC} into the phase modulator, and the results are shown in Fig. 9. This demonstrates a continuous $-180°$ to 180° phase shift with a flat

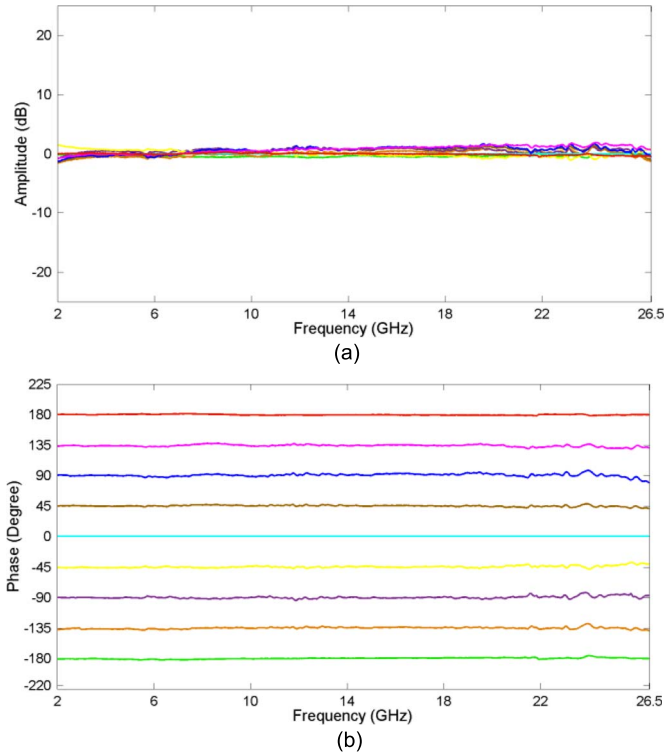

Fig. 9. Measured DP-DPMZM and OPS based microwave photonic phase controller (a) amplitude and (b) phase response for different DC voltages into the phase modulator.

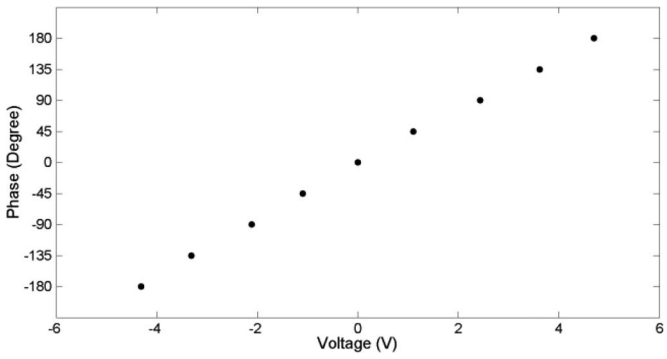

Fig. 10. Experimentally measured RF signal phase shift as a function of DC voltage into the phase modulator.

phase and amplitude response performance over a wide range of frequency. The measurements show < 9° phase deviation and < 3.6 dB amplitude variation over 2–26.5 GHz frequency range, which is limited by the bandwidth of the 90° hybrid coupler. The measured phase controller phase and amplitude variation were mainly due to the 90° hybrid coupler phase and amplitude imbalance, and are agreed with the simulation results shown in Fig. 5. Fig. 10 shows a total of 8.9 V DC voltage is needed to achieve the full −180° to 180° RF signal phase shift. It also demonstrates the phase controller has a linear RF signal phase shift to control voltage relationship.

Finally, the 2–26.5 GHz bandwidth 90° hybrid coupler used in the experiment was replaced by a 0.5–9 GHz bandwidth 90° hybrid coupler to show the phase controller not only can operate at high frequencies but also at low frequencies. Fig. 11 shows the phase controller exhibits a

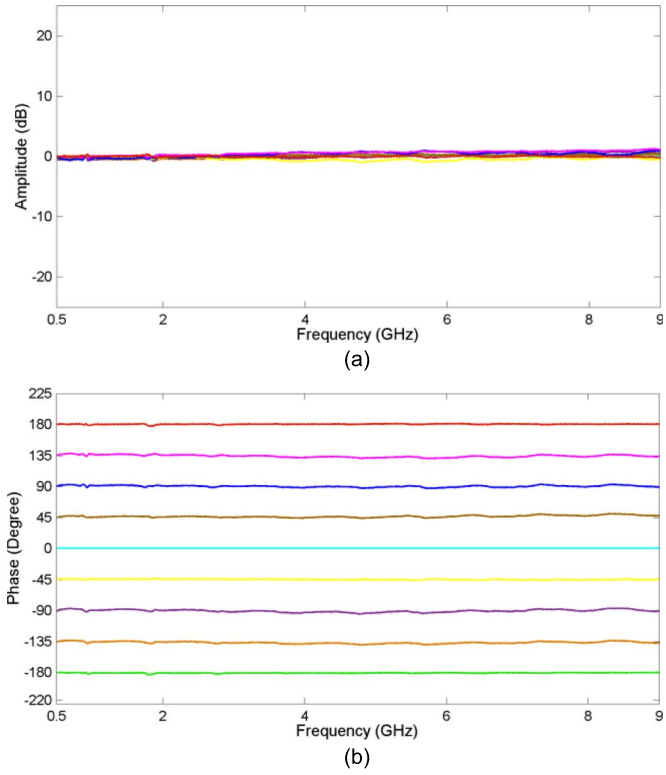

Fig. 11. Measured DP-DPMZM and OPS based microwave photonic phase controller (a) amplitude and (b) phase response for different DC voltages into the phase modulator when a 0.5 to 9 GHz bandwidth 90° hybrid coupler is used to generate a pair of 90° phase difference RF signals.

flat phase and amplitude response over the 0.5–9 GHz frequency range when the 0.5–9 GHz bandwidth 90° hybrid coupler was used to generate a pair of 90° phase difference RF signals into the DP-DPMZM. The amount of DC voltage needed to achieve the full −180° to 180° RF signal phase shift was 8.8 V, which is similar to that when using the 2–26.5 GHz bandwidth 90° hybrid coupler. The phase and amplitude variation over the measurement frequency range of 0.5–9 GHz were < 4° and < 2.3 dB, respectively. Using the measured 90° hybrid coupler ±1.4° phase imbalance and ±0.7 dB amplitude imbalance, simulation results show the phase controller has < 2.4° phase deviation and < 1.3 dB amplitude variation, which are agreed with the measurements. This shows the phase controller phase and amplitude variation are determined by the 90° hybrid coupler phase and amplitude imbalance, and a 90° hybrid coupler with low phase and amplitude imbalance can be used to improve the flatness of the phase controller phase and amplitude response.

6. Conclusion

A novel microwave photonic signal processor for RF phase controlling operation has been presented. It is based on a DP-DPMZM and a polarization dependent OPS. It can realize a continuously tunable 0° to 360° phase shift with high resolution. The phase controller has a fast tuning time, a simple structure, and requires only one DC voltage control. It can easily be extended to obtain multiple RF signal phase shifts suitable for beamforming applications. Experimental results demonstrate a −180° to 180° RF phase controlling operation with a flat phase and amplitude response performance over 2–26.5 GHz frequency range, and results demonstrate the RF signal phase shift and the control voltage has a linear relationship. The phase controller phase and amplitude variation have been investigated, and the measurements are agreed with the simulation results.

Acknowledgment

The authors gratefully acknowledge Mr. Y. Chen from PlugTech for valuable discussions.

References

[1] W. Liu and S. Weiss, *Wideband Beamforming: Concepts and Techniques*. Chichester, U.K.: Wiley, 2010.
[2] G. M. Rebeiz, G. L. Tan, and J. S. Hayden, "RF MEMS phase controllers: Design and applications," *IEEE Microw. Mag.*, vol. 3, no. 2, pp. 72–82, Jun. 2002.
[3] C. F. Campbell and S. A. Brown, "A compact 5-bit phase-controller MMIC for K-band satellite communication systems," *IEEE Trans. Microw. Theory Tech.*, vol. 48, no. 12, pp. 2652–2656, Dec. 2000.
[4] F. Ellinger, U. Lott, and W. Bächtold, "A calibratable adaptive antenna combiner at 5.2 GHz with high yield for PCMCIA card integration," *IEEE Trans. Microw. Theory Tech.*, vol. 48, no. 12, pp. 2714–2720, Dec. 2000.
[5] H. Hayashi and M. Muraguchi, "An MMIC active phase controller using a variable resonant circuit," *IEEE Trans. Microw. Theory Tech.*, vol. 47, no. 10, pp. 2021–2026, Oct. 1999.
[6] K. J. Koh and G. M. Rebeiz, "A 6–18 GHz 5-bit active phase controller," in *Proc. IEEE MTT-S Int. Microw. Symp. Dig.*, May 2010, pp. 792–795.
[7] R. A. Minasian, E. H. W. Chan, and X. Yi, "Microwave photonic signal processing," *Opt. Exp.*, vol. 21, no. 19, pp. 22918–22936, Sep. 2013.
[8] E. H. W. Chan, W. Zhang, and R. A. Minasian, "Photonic RF phase controller based on optical carrier and RF modulation sidebands amplitude and phase control," *J. Lightw. Technol.*, vol. 30, no. 23, pp. 3672–3678, Oct. 2012.
[9] X. Wang, E. H. W. Chan, and R. A. Minasian, "All-optical microwave photonic phase controller based on an optical filter with a nonlinear phase response," *J. Lightw. Technol.*, vol. 31, no. 20, pp. 3323–3330, Sep. 2013.
[10] W. Li, W. H. Sun, W. T. Wang, and N. H. Zhu, "Optically controlled microwave phase controller based on nonlinear polarisation rotation in a highly nonlinear fibre," *Opt. Lett.*, vol. 39, no. 11, pp. 3290–3293, Jun. 2014.
[11] E. H. W. Chan and R. A. Minasian, "Photonic RF phase controller and tunable photonic RF notch filter," *J. Lightw. Technol.*, vol. 24, no. 7, pp. 2676–2682, Jul. 2006.
[12] X. Xue, X. Zheng, H. Zhang, and B. Zhou, "Tunable 360° photonic radio frequency phase controller based on optical quadrature double-sideband modulation and differential detection," *Opt. Lett.*, vol. 36, no. 23, pp. 4641–4643, Dec. 2011.
[13] A. Loayssa and F. J. Lahoz, "Broad-band RF photonic phase controller based on stimulated Brillouin scattering and signal-sideband modulation," *IEEE Photon. Technol. Lett.*, vol. 18, no. 1, pp. 208–210, Jan. 2006.
[14] W. Li, N. H. Zhu, and L. X. Wang, "Photonic phase controller based on wavelength dependence of Brillouin frequency shift," *IEEE Photon. Technol. Lett.*, vol. 23, no. 14, pp. 1013–1015, Jul. 2011.
[15] M. Pagani, D. Marpaung, D. Y. Choi, S. J. Madden, B. L. Davies, and B. J. Eggleton, "Tunable wideband microwave photonic phase controller using on-chip stimulated Brillouin scattering," *Opt. Exp.*, vol. 22, no. 23, pp. 28810–28818, Nov. 2014.
[16] X. Wang, J. Yang, E. H. W. Chan, X. Feng, and B. Guan, "Microwave photonic phase controller based on dual-sideband phase-control technique," *Opt. Lett.*, vol. 40, no. 15, pp. 3508–3511, Aug. 2015.
[17] J. Yang, E. H. W. Chan, X. Wang, X. Feng, and B. Guan, "Broadband microwave photonic phase controller based on controlling two RF modulation sidebands via a Fourier-domain optical processor," *Opt. Exp.*, vol. 23, no. 9, pp. 12100–12110, May 2015.
[18] S. Pan and Y. Zhang, "Tunable and wideband microwave photonic phase controller based on a signal-sideband polarisation modulator and a polariser," *Opt. Lett.*, vol. 37, no. 21, pp. 4483–4485, Nov. 2012.
[19] J. Shen, G. Wu, W. Zou, and J. Chen, "A photonic RF phase controller based on a dual-parallel Mach–Zehnder modulator and an optical filter," *Appl. Phys. Exp.*, vol. 7, no. 5, pp. 0725021–0725024, Jul. 2014.
[20] Y. Zhang, H. Wu, D. Zhu, and S. Pan, "An optically controlled phase array antenna based on signal sideband polarisation modulation," *Opt. Exp.*, vol. 22, no. 4, pp. 3761–3765, Feb. 2014.
[21] X. Wang, E. H. W. Chan, and R. A. Minasian, "Optical-to-RF phase shift conversion-based microwave photonic phase controller using a fibre Bragg grating," *Opt. Lett.*, vol. 39, no. 1, pp. 142–145, Jan. 2014.
[22] W. Li, W. T. Wang, and N. H. Zhu, "Broadband microwave photonic splitter with arbitrary amplitude ratio and phase shift," *IEEE Photon. J.*, vol. 6, no. 6, Dec. 2014, Art. no. 5501507.
[23] S. Shimotsu *et al.*, "Single side-band modulation performance of a $LiNbO_3$ integrated modulator consisting of four-phase modulator waveguides," *IEEE Photon. Technol. Lett.*, vol. 13, no. 4, pp. 364–366, Apr. 2001.
[24] *Keysight N7784B High Speed Polarisation Controller*. [Online]. Available: http://www.keysight.com
[25] *PlugTech Ultra Compact DP-IQ Modulator Bias Controller*. [Online]. Available: http://plugtech.hk/data/documents/MBC-DPIQ-ENG.pdf
[26] C. H. Lee, *Microwave Photonics*. Boca Raton, FL, USA: CRC, 2007.
[27] S. K. Mathew, "Experimentally determined r_{13} electro-optic coefficient for a lithium niobate crystal," *App. Opt.*, vol. 42, no. 18, pp. 3580–3582, Jun. 2003.
[28] A. Petris *et al.*, "The r_{33} electro-optic coefficient of Er:$LiNbO_3$," *J. Opt.*, vol. 12, Jan. 2010, Art. no. 015205.
[29] *VPItransmissionMaker Photonic Simulator*. [Online]. Available: www.VPIsystems.com
[30] *Marki Microwave 3 dB Quadrature (90 degree) Hybrid*. [Online]. Available: http://www.markimicrowave.com